Vol 16 No 3, March 2007
1009-1963/2007/16(03)/0817-04

Chinese Physics

© 2007 Chin. Phys. Soc.
and IOP Publishing Ltd

Comparison of two kinds of active layers for high-power narrow-stripe distributed feedback laser diodes*

Fu Sheng-Hui(付生辉)†, Song Guo-Feng(宋国峰), and Chen Liang-Hui(陈良惠)

Institute of Semiconductors, Chinese Academy of Sciences, Beijing 100083, *China*

(Received 4 July 2006; revised manuscript received 5 August 2006)

Usually GaAs/AlGaAs is utilized as an active layer material in laser diodes operating in the spectral range of 800–850 nm. In this work, in addition to a traditional unstrained GaAs/AlGaAs distributed feedback (DFB) laser diode, a compressively strained InGaAlAs/AlGaAs DFB laser diode is numerically investigated in characteristic. The simulation results show that the compressively strained DFB laser diode has a lower transparency carrier density, higher gain, lower Auger recombination rate, and higher stimulated recombination rate, which lead to better a device performance, than the traditional unstrained GaAs/AlGaAs DFB laser diode.

Keywords: InGaAlAs/AlGaAs, distributed feedback laser diode, numerical simulation
PACC: 7280E, 0365, 6120J

1. Introduction

High-power, single-mode distributed feedback (DFB) laser diodes have important applications in communication, spectroscopy, and frequency conversion.[1−3] DFB laser diodes are superior to conventional Fabry–Perot (FP) laser diodes in spectral purity and modal stability. DFB laser diodes with an InGaAlAs/AlGaAs active region are attractive as high-power devices operating in the spectral range of 800–850 nm. The quarternary InGaAlAs active region seems to have distinct advantages over the traditional GaAs quantum well construction. It allows the fabrication of devices that work at wavelengths not feasible by means of lattice-matched growth. Furthermore, it has been shown that for some kinds of devices, the strain in the material enables us to make better devices due to the beneficial influence of the strain on the band structure.[4]

In this work, we have modelled a single quantum well graded-index separate confinement heterostructure (GRIN-SCH) DFB laser diode using advanced 3D laser simulation software.[5] For a DFB laser diode, 3D simulation is needed due to the z-direction variation (longitudinal spatial hole-burning effect, etc). The basic equations that describe the electrical behaviour of semiconductor are Poisson's equation and the current continuity equations for electrons and holes. To account for the optical properties of a semiconductor laser, i.e. the optical field distribution and photon number in the laser cavity, both the complex scalar wave equation, and the photon rate equation are solved. The optical gain is calculated based on the interband transition model. Strained quantum wells are treated using the $4 \times 4\,\boldsymbol{k}\boldsymbol{p}$ theory including valence band mixing. Carrier losses due to Auger recombination, spontaneous emission, Shockley–Read–Hall (SRH) and leakage (vertical and lateral) recombination are considered. The grating-related calculations are based on coupled wave equations, with the Green function method incorporated. A detailed description of the model can be found in the PICS3D user's manual.[5]

2. Device structure and simulation parameters

The DFB laser diode under consideration consists of an n-GaAs buffer, an n-$Al_{0.42}Ga_{0.58}As$ cladding, a 70 nm $Al_xGa_{1-x}As$ (x: $0.42 - 0.2$) waveguide, a 7 nm InGaAlAs or GaAs active quantum well (QW) sandwiched by 15nm $Al_{0.2}Ga_{0.8}As$ barriers, a 70 nm $Al_xGa_{1-x}As$ (x: $0.2 - 0.42$) waveguide, an InGaP second-order grating layer (triangular-shaped, period 244 nm, depth 30nm with an assumed duty-cycle of

*Project supported by the National Natural Science Foundation of China (Grant No 10374085).
†E-mail: fushenghui@red.semi.ac.cn

0.75), a 100nm $Al_{0.2}Ga_{0.8}As$ layer, a p-$Al_{0.42}Ga_{0.58}As$ cladding, and a p-GaAs contact layer. Lateral optical confinement is provided by a narrow-stripe ridge waveguide (assumed to be 3 μm wide).

Material-dependent parameters such as bandgap, effective masses, etc. (and their temperature dependence) are cited from Ref.[5]. For simplicity, a temperature-independent radiative recombination coefficient $B = 1 \times 10^{-10}$ cm^3/s[6] is used. Similarly, temperature-independent Auger coefficients are set to be $C_n = C_p = 2 \times 10^{-30}$ cm^6/s[5] for the whole structure. The conduction band offset ratio ($\Delta E_c/\Delta E_g$) is set as 67% [7] and 65%[8] for the compressively strained InGaAlAs/AlGaAs quantum well structure and unstrained GaAs/AlGaAs quantum well structure, respectively. The intraband scattering time is assumed to be 0.1 ps [9,10] in calculation, and a typical internal loss value of 5 cm^{-1} is adopted.

3. Results and discussion

Our goal is to compare the performance of a 0.65% compressively strained InGaAlAs/AlGaAs laser with that of a traditional unstrained GaAs/AlGaAs laser.

Figure 1 shows the calculated valence band structures for the two materials considered. The InGaAlAs/AlGaAs quantum well structure has fewer confined hole levels. That is, in the InGaAlAs/AlGaAs quantum well structure there exist two heavy hole (HH) levels and one light hole (LH) level while three heavy hole (HH) levels and two light hole (LH) levels occur in the GaAs/AlGaAs quantum well. The number of confined hole levels may be influenced by the amount of strain in the QW and the effective masses of electrons and holes. It also can be seen that the separation between HH and LH is obvious due to the compressive strain in the quantum well. Note that the strength of the TM mode is mainly provided by the C1-LH1 transitions. However, the compressive strain lowers the LH1 band away from the valence band edge. The above two factors have a positive influence on the gain and transparency carrier density as shown in Fig.2.

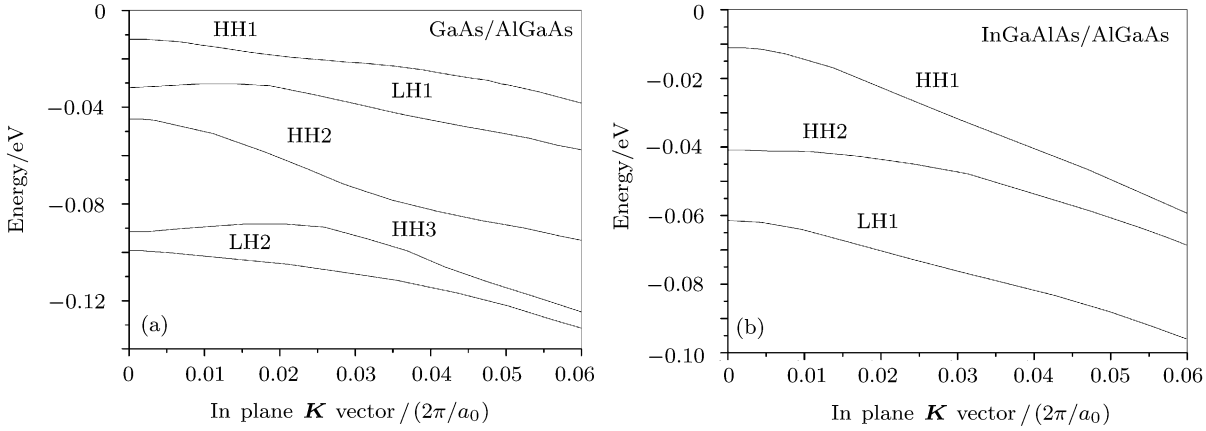


Fig.1. (a) The valence subband structures with $a_0 = 5.653$ Å (b) and for GaAs/AlGaAs quantum well structure with $a_0 = 5.653$ Å .

Figure 2 shows the peak material gains as a function of carrier densities of the GaAs and InGaAlAs QWs with an $Al_{0.2}Ga_{0.8}As$ barrier at (a) $T = 300$ K and (b) $T = 370$ K. The transparency carrier density of the InGaAlAs/AlGaAs quantum well structure is lower than that of the GaAs/AlGaAs quantum well structure at both temperatures. The transparency carrier density depends primarily on the band curvature, which is sensitive to the effective mass and the amount of strain. In this study, it is shown that the transparency carrier density of the GaAs QW increases by approximately 34% as the temperature increases from 300 to 370 K. For the InGaAlAs QW, the transparency carrier density increased by 28% as the temperature increases from 300 to 370 K, which is smaller than that of the GaAs QW because compressive strain in the QW can reduce the transparency carrier density and the relatively large conduction band offset can prevent carriers from escaping from the QW.

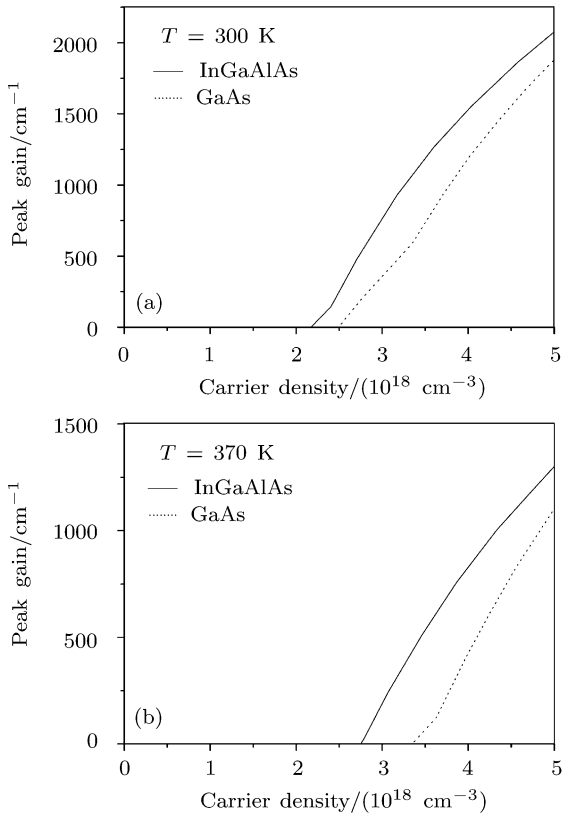


Fig.2. Plot of peak material gain as a function of carrier density at 300 K (a) and at 370 K (b).

Figures 3 and 4 show the Auger recombination rates and stimulated recombination rates in the QWs of the two structures, respectively with an input current of 200 mA. It is obviously shown from Figs.3 and 4 that the InGaAlAs/AlGaAs quantum well structure has a higher stimulated emission rate and its Auger recombination rate is much smaller than that of the GaAs/AlGaAs quantum well structure. That means that the nonradiative recombination of the InGaAlAs/AlGaAs quantum well structure is less severe than that of the GaAs/AlGaAs quantum well structure. Hence a better laser performance can be expected. In addition, the increase of transparency carrier density with the increase of temperature as shown in Fig 2 is attributed to the increment of nonradiative recombination and the poor electron confinement; namely, a large number of electrons can pile up from the QW and overflow when the temperature is high. Therefore, as shown in the insets of Figs.3 and 4, there is an increase in the Auger recombination rate and a decrease in the stimulated recombination rate at a higher temperature (370 K) as compared with the case at 300 K, regardless of the difference between the quantum well structures. Furthermore, on the one hand, the Auger recombination rate of the InGaAlAs/AlGaAs QW structure at a higher temperature (370 K) is even smaller than that of the GaAs/AlGaAs QW structure at a relatively low temperature (300 K), on the other hand, as the temperature increases from 300 to 370 K, the stimulated recombination rate of the InGaAlAs/AlGaAs QW structure decreases by only 4.5% while that of the GaAs/AlGaAs QW structure decreases by 24%. Hence a better laser performance with InGaAlAs/AlGaAs quantum well structure at high temperatures can also be expected.

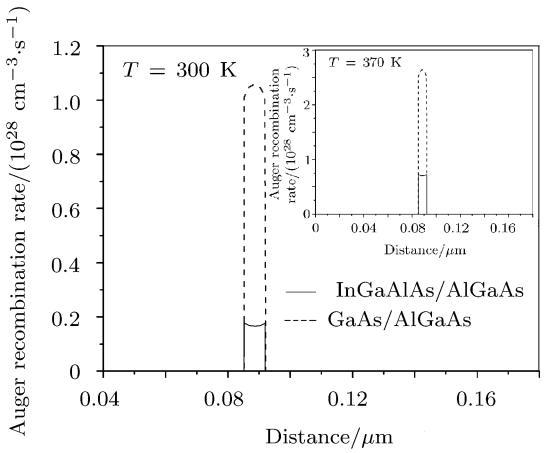


Fig.3. Auger recombination rates in the two QWs under study.

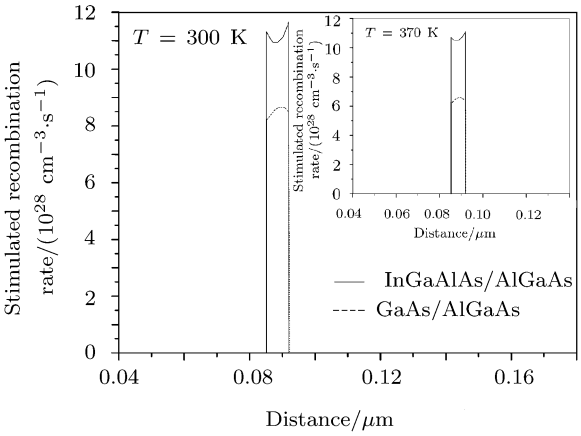


Fig.4. Stimulated recombination rates in the two QWs under study.

Figure 5 shows the laser output power as a function of input current at 300 K for the two DFB laser structures under study. Crystal defects (SRH recombination) and the Auger process cause nonradiative recombination. Photos are generated by spontaneous and stimulated recombinations. Carriers may also leak out of the separate confinement layer. Carriers leaving the ridge waveguide region (the 3 μm wide

ridge waveguide assumed in our simulation) are eventually recombined; however, they are considered as leakage carriers in our analysis. Recombinations inside the waveguide region plus both of the leakage currents add up to the total injection current. The threshold current compensates for all of the carrier losses mentioned above at the lasing threshold.[11] The InGaAlAs/AlGaAs and GaAs/AlGaAs QW structures have the threshold currents of 18 mA and 42 mA, respectively. When the input current is 200 mA, the laser output power of the InGaAlAs/AlGaAs DFB laser is 75mW, which is almost 23% larger than that of the GaAs/AlGaAs DFB laser.

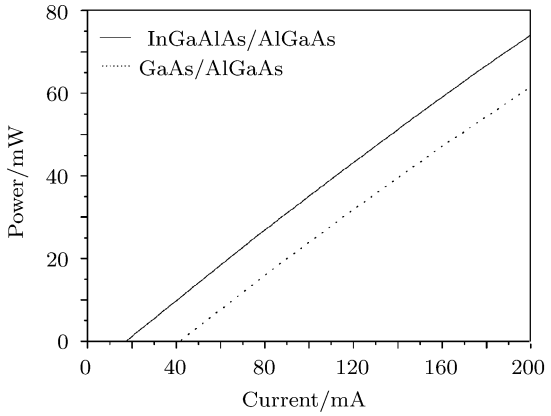


Fig.5. Output power–current characteristics for the two DFB laser structures under study.

In a CW operation, another main variable concerned of DFB laser diodes is the side mode suppression Ratio (SMSR). It is well known that the coupling coefficient and spatial hole-burning affect the SMSR. Figure 6 shows the SMSR as a function of input current for the two DFB laser structures under study. The SMSR increases abruptly near the laser threshold and levels off at higher currents due to the spatial hole-burning effect. It is also indicated from Fig.6 that the InGaAlAs/AlGaAs DFB laser has a larger SMSR than the GaAs/AlGaAs DFB laser for all current input levels, which is beneficial to single laser mode operation.

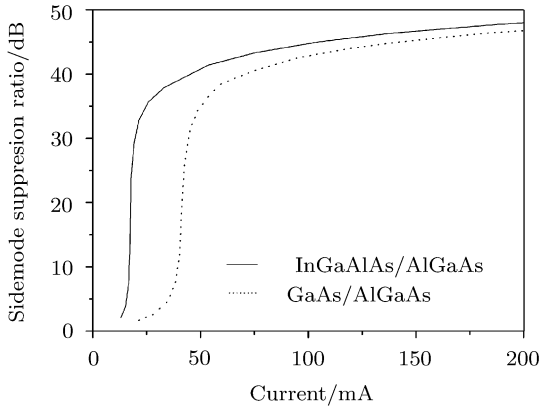


Fig.6. SMSR for the two DFB laser structures under study.

4. Conclusion

We have numerically investigated the characteristics of a traditional unstrained GaAs/AlGaAs DFB laser diode and a compressively strained InGaAlAs/AlGaAs DFB laser diode. The simulation results show that the compressively strained DFB laser diode has a better optical performance than that of the traditional unstrained GaAs/AlGaAs DFB laser diode.

Acknowledgment

The authors would like to thank the members of the nano-opotoelectronics laboratory for helpful discussion.

References

[1] Wang C L, Wu J and Lin J T 2003 *Chin. Phys.* **12** 528

[2] Zhao Q, Pan J Q, Zhang J, Li B X, Zhou F, Wang B J, Wang L F, Bian J, Zhao L J and Wang W 2006 *Acta Phys. Sin.* **55** 1259 (in Chinese)

[3] Fu S H, Zhong Y, Song G F and Chen L H 2006 *Chin. J. Semicond.* **27** 966 (in Chinese)

[4] Keisuke K, Susumu N and Kazumasa M 1986 *J. Lightwave Technol.* **4** 507

[5] PICS3D trail version Crosslight Inc. Software Canada Available online at http://www.crosslight.ca

[6] Yu S F, Wong W N, Shum P and Li E H 1996 *IEEE J. Quantum Electron.* **32** 2139

[7] Jensen J R, Hvam J M and Langbein W 1999 *J. Appl. Phys.* **86** 2584

[8] Joachim P 2003 *Semiconductor Optoelectronic Devices* (San Francisco: Academic) p48

[9] Ahn D, Chuang S L and Chang Y C 1988 *J. Appl. Phys.* **64** 4056

[10] Ahn D and Chuang S L 1990 *IEEE J. Quantum Electron.* **26** 13

[11] Joachim P 2003 *Semiconductor Optoelectronic Devices* (San Francisco: Academic) p154